

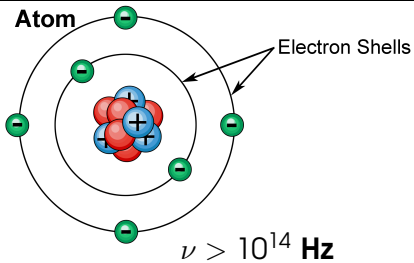
# Overview of $^{229m}\text{Th}$ based nuclear clock

M. Osipenko<sup>1</sup>

<sup>1</sup>INFN Genova

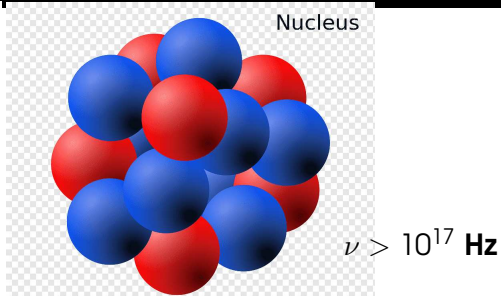
The Low Energy Frontier of Particle Physics,  
Frascati, 12 February 2025

# Atomic and nuclear scales



**Radius:** 0.5-2 Å (0.1 nm)  
**Excitations:** eV - keV

- *highly monochromatic coherent lasers (eV),*
- *visible-microwave comb ( $\frac{\Delta\nu}{\nu} \sim 10^{-18}$ ),*
- *optical ion clocks:  $Yb^+$ ,  $Al^+$ ,  $Ca^+$ ,  $Sr^+$ ,  $Hg^+$  etc,*
- *1 s≡9.192.631.770 RF oscillations in Cs clock.*

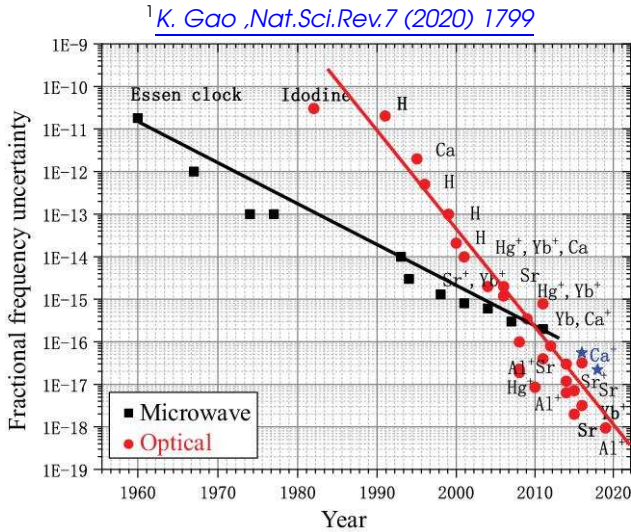


**Radius:** 1.3-8 fm ( $10^{-6}$  nm)  
**Excitations:** keV - MeV

- *incoherent  $\gamma$ -sources,*
- *broad linewidth FELs ( $\frac{\Delta\nu}{\nu} \sim 10^{-3} \div 10^{-5}$ ),*
- *Mössbauer spectroscopy ( $\frac{\Delta\nu}{\nu} > 10^{-22}$ ),*
- *no link to RF electronics.*

# Atomic clock evolution

- 1 Cs atomic fountain  
- J. Zacharias 1956,
- 2 GPS application  
- 1978/1993,
- 3 optical ion clock -  
H.G. Dehmelt and  
W. Paul  
Nobel Prize 1989,
- 4 laser cooling -  
S. Chu, C. Cohen  
and W.D. Phillips  
Nobel Prize 1997,
- 5 visible-microwave  
comb - Th. Hänsch  
and J. Hall  
Nobel Prize 2005.



# Atomic clock precision

<sup>1</sup>K. Gao ,*Nat.Sci.Rev.*7 (2020) 1799

- ① Black Body Radiation (BBR),
- ② servo frequency steering,
- ③ 2d order Doppler shift,
- ④ electric quadruple shift,
- ⑤ Zeeman shift,
- ⑥ Stark shift.

The Ca<sup>+</sup>-clock systematic-uncertainty budget table (unit in 10<sup>-18</sup>).

Contribution	Fractional frequency shift	Fractional frequency uncertainty
BBR field evaluation (temperature)	863	19
BBR coefficient ( $\Delta\alpha_0$ )	0	0.3
Excess micromotion	0	0.4
Second-order Doppler (thermal)	-5.0	2.5
ac Stark shift	1.2	1.3
Residual quadrupole	0	2.3
Zeeman effect	0	1.5
Servo	0.0	3.0
Total	859	20

# Nuclear clock precision

First idea from: [E.V. Tkalya et al., Phys. Scr. 53, 296 \(1996\).](#),  
[E. Peik and C. Tamm, Eur.Phys.Lett.61, 181 \(2003\),](#)

- the same technique as in optical atomic clocks,
- small coupling of external fields to nucleus,
- atomic shell screening,
- **small black-body radiation uncertainty.**

Type of shift	Shift ( $\times 10^{-20}$ )	Uncertainty ( $\times 10^{-20}$ )
Excess micromotion	10	10
Gravitational	0	10
Cooling laser stark	0	5
Electric quadrupole	3	3
Secular motion	5	1
Linear Doppler	0	1
Linear Zeeman	0	1
Collisions	0	1
Blackbody radiation	0.013	0.013
Clock laser stark	0	$\ll 0.01$
Trapping field stark	0	$\ll 0.01$
Quadratic Zeeman	0	0
Total	18	15

<sup>1</sup> [C.J. Campbell et al., Phys.Rev.Lett. 108 \(2012\) 120802](#)

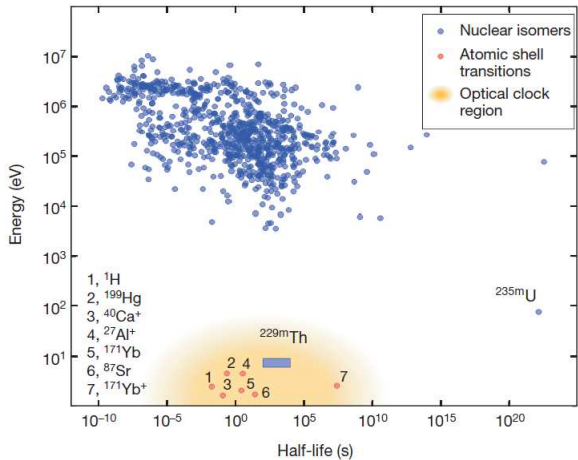
# Known nuclear isomers

Need an isomer with long lifetime and large energy:

$$\frac{\Delta\nu}{\nu} = \frac{\Gamma_m}{E_m} = \ln(2) \frac{\hbar}{E_m t_{1/2}} = \frac{4.6 \times 10^{-16}}{\frac{E_m}{\text{eV}} \frac{t_{1/2}}{\text{s}}} < 10^{-19}$$

- 1  $^{229m}\text{Th}$  at 8 eV  
with half life 7  $\mu\text{s}$   
(IC) or 1 hour ( $\gamma$ ),
- 2  $^{235m}\text{U}$  at 76.8 eV  
with half life  
25 min. (IC) or  
 $10^{14}$  years ( $\gamma$ ).

All other known  
nuclear isomers have  
energy  $> 1 \text{ keV}$ .



## $^{229m}\text{Th}$ isomer - optical range nuclear level

- 43 years from the first indication based on level scheme to the final confirmation,
- resurgence of interest due to **nuclear clock**
- several multi M€ projects in EU:  
nuClock FET (2015-2019) 4 MEuro;  
ThoriumNuclearClock ERC (2020-2026) 14 MEuro.
- $\gamma$ -decay (dominant IC) recently observed,
- photo-induced excitation of  $^{229m}\text{Th}$  recently observed.

Year	Energy (eV)	Ref.
1976	<100	L.A. Kroger, C.W. Reich, Nucl.Phys. <b>A259</b> , 29
1990	$1 \pm 4$	C.W. Reich, R. Helmer, Phys.Rev.Lett. <b>64</b> , 271
1994	$3.5 \pm 1$	R. Helmer, C.W. Reich, Phys.Rev. <b>C49</b> , 1845
2007	$7.6 \pm 0.5$	B.R. Beck <i>et al.</i> , Phys.Rev.Lett. <b>109</b> , 142501
2019	$8.3 \pm 0.2$	B. Seiferle <i>et al.</i> , Nature <b>573</b> , 243
2023	$8.34 \pm 0.02$	S. Kraemer <i>et al.</i> , Nature <b>617</b> , 706

# Non-spherical $^{229}\text{Th}$ rotational splitting

- 1  $^{229}\text{Th}$  deformed nucleus (axial),



- 2 Nilsson model<sup>1</sup> level scheme<sup>2</sup>:

$$E(\Omega^\pi[N, n_z, \Lambda]) ,$$

$$\Omega = j_z, [2j + 1]$$

$$N = n_z + n_\perp$$

$$\Lambda = l_z, [2n_\perp + 1]$$

- 3 deformation parameter:

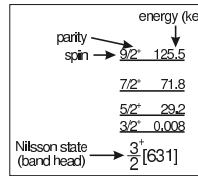
$$\delta = 1 - \left( \frac{L_\perp}{L_z} \right)^2$$

- 4  $^{229}\text{Th}$  prolate<sup>3,4,5</sup>

$$\delta \sim 0.1, L_z \sim 1.05 L_\perp$$

$$M1\left(\frac{3}{2}^+ \rightarrow \frac{5}{2}^+\right)$$

$Q > 0$	Prolate	$\frac{5}{2}^+$ 605.3 $\frac{3}{2}^+$ 569.3 $\frac{3}{2}^-$ [642]	$\frac{5}{2}^+$ 478.6 $\frac{3}{2}^+$ 425.3 $\frac{1}{2}^-$ [743]	$\frac{1}{2}^-$ 53
		$\frac{7}{2}^+$ 303.0 $\frac{7}{2}^-$ [613]	$\frac{7}{2}^+$ 317.2 $\frac{3}{2}^+$ 288.5 $\frac{1}{2}^+$ 262.0 $\frac{5}{2}^+$ [622]	$\frac{7}{2}^+$ 465.4 $\frac{7}{2}^-$ [770]
		$\frac{11}{2}^+$ 162.8 $\frac{9}{2}^+$ 97.1 $\frac{7}{2}^+$ 42.3 $\frac{5}{2}^+$ 0.0	$\frac{7}{2}^+$ 148.2 $\frac{5}{2}^+$ 146.4 $\frac{5}{2}^+$ 29.2 $\frac{3}{2}^+$ 0.008 $\frac{5}{2}^+$ [633] $\frac{3}{2}^+$ [631]	$\frac{3}{2}^+$ 164.5 $\frac{3}{2}^+$ [761] $\frac{5}{2}^+$ [752] $\frac{3}{2}^+$ [631]
				$\Delta I_z = 1$ band splitting



<sup>1</sup>S.Nilsson,*Matematisk-fysiske Meddelelser*,29(16)(1955)

<sup>2</sup>G.Musiol et al.,*Kern und El.physik.*,Weinheim(1988)

<sup>3</sup>E.Ruchowska et al.,*Phys.Rev.C*73,044326(2006).

<sup>4</sup>A.Hayes et al.,*Phys.Rev.C*78,024311(2008).

<sup>5</sup>E.Litvinova et al.,*Phys.Rev.C*79,064303(2009).

# $^{229m}\text{Th}$ isomer decays

- ① magnetic dipole transition M1:  $\frac{3}{2}^+ \rightarrow \frac{5}{2}^+$ , with decay  $\gamma$  angular distribution  $(1+\cos\theta_\gamma)$ ,
- ② calculated lifetime<sup>1,2,3</sup> ( $\gamma$  only):

$$\tau_\gamma \sim \frac{10.95h}{E_\gamma^3 B(M1)} \sim 1h, \quad B(M1) \sim 0.025\mu_N^2$$

- ③ ionization energy of 6.5 eV shortens the lifetime (IC) to 7  $\mu\text{s}$  in neutral atom<sup>4</sup>, ( $\Delta\nu/\nu \sim 10^{-11}$  not suitable for nuclear clock, requiring  $\Delta\nu/\nu < 10^{-16}$ ),
- ④ ionized or bound  $\text{Th}^+$  ion suppresses IC-decay branch,
- ⑤ in  $\text{MgF}_2$  ( $n=1.488$ ) crystal measured lifetime of  $967 \pm 147 \text{ s}$ <sup>5</sup> in agreement with calculations including  $1/n^3$ -scaling<sup>6</sup>:  $967 \text{ s} \times n^3 \sim 1 \text{ h}$ .

<sup>1</sup>R.Helmer and C.Reich. Phys.Rev.C49, 1845(1994).

<sup>2</sup>V.Strizhov and E.Tkalya. Sov.Phys.JETP72, 387(1991).

<sup>3</sup>E.Ruchowska et al., Phys.Rev.C73, 044326(2006).

<sup>4</sup>B.Seiferle et.al.Phys.Rev.Lett. 118, 042501(2017).

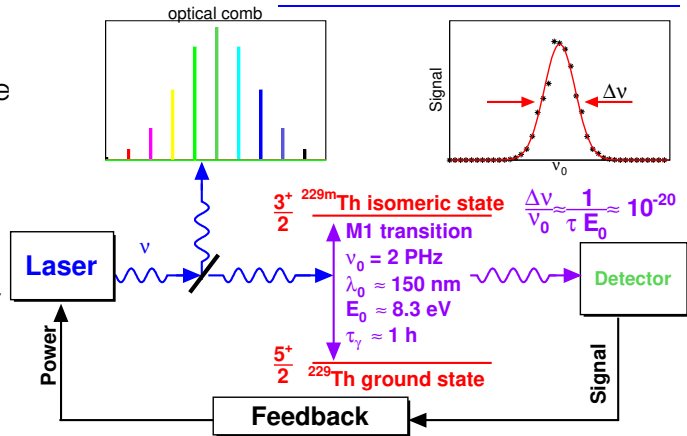
<sup>5</sup>S.Kraemer et al.Nature 617, 706 (2023).

<sup>6</sup>E.V. Tkalya et al., Phys.Rev.C61, 064308(2000).

# $^{229}\text{Th}$ -based Nuclear Clock

- 1 Lowest nuclear excited state<sup>1</sup>,
- 2 dominant IC decay<sup>2</sup> can be suppressed,
- 3 VUV-laser excitation,
- 4  $\gamma$ -linewidth  $\Delta\nu \sim 0.1 \text{ mHz}^3$ ,
- 5  $N = 10^5 \div 10^{12}$  oscillators<sup>4,5</sup>,  
$$\text{FoM} = \frac{\nu\sqrt{N}}{\Delta\nu},$$
- 6  $>10^1 \div 10^2$  FoM improvement wrt atomic clock.

N. Poli et al., Nuov. Cim. 36 (2013) 555



<sup>1</sup> L. Kroger and C. Reich, Nucl. Phys. A259, 29 (1976).

<sup>2</sup> B. Seiferle et al., Nature 573, 243 (2019).

<sup>3</sup> V. Strizhov and E. Tkalya, Sov. Phys. JETP 72, 387 (1991).

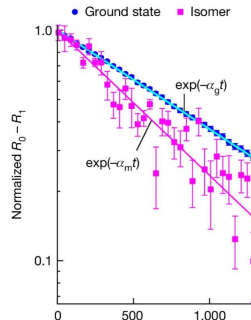
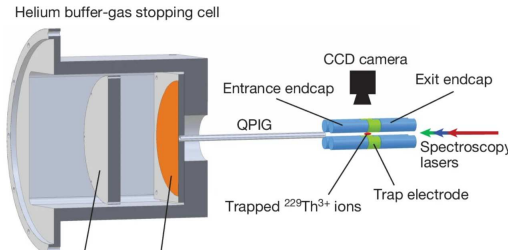
<sup>4</sup> C. Campbell et al., Phys. Rev. Lett. 102, 233004 (2009).

<sup>5</sup> R. Jackson et al., J. Phys. Cond. Mat. 21, 325403 (2009).

# $^{229}\text{Th}^{3+}$ $\gamma$ -decay

- ① 2000  $^{229}\text{Th}^{3+}$  ions/s in linear Paul trap (40%, 15 min.),
- ② laser spectroscopy around  $6\text{d}^2\text{D}_{5/2} \rightarrow 5\text{f}^2\text{F}_{7/2}$  (984 nm),
- ③ hyperfine constants of magnetic dipole and electric quadrupole of the  $6\text{d}^2\text{D}_{5/2}$  state were determined,
- ④ magnetic dipole and electric quadrupole moments of  $^{229m}\text{Th}$  were determined to be  $-0.378(8)\mu_N$  and  $8.84(10)$  eb, respectively,
- ⑤  $^{229m}\text{Th}^{3+}$  half-life  $\tau_\gamma = 1400^{+600}_{-300}$  s was measured.

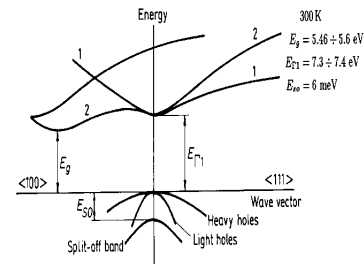
A.Yamaguchi et al., Nature 629 (2024) 62,



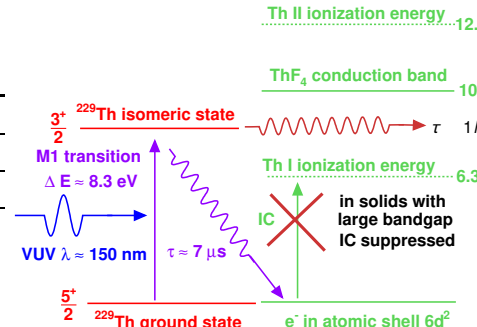
# Chemical bonding IC suppression

- 1 IC decay requires:  
 $E_{decay} > E_{gap}$ ,
- 2 find Th-compound with  
 $E_{gap} > 8.3 \text{ eV}$ ,
- 3 theoretical calculations<sup>1</sup>  
suggested  $\text{Na}_2\text{ThF}_6$  and  $\text{ThF}_4$   
would have  $E_{gap} > 8.9 \text{ eV}$ ,  
while  $\text{ThX}_4$  ( $X=\text{Cl}, \text{Br}, \text{I}$ )  
 $E_{gap} < 6.5 \text{ eV}$ .

Comp.	Bandgap (eV)
$\text{CaF}_2^t$	12
$\text{UO}_2$	2.2
UC,UN,UCI,UF	2-3
Other	?



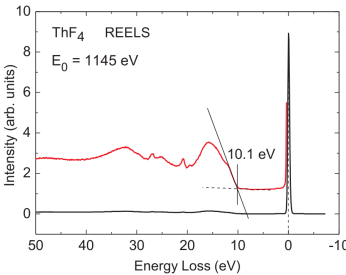
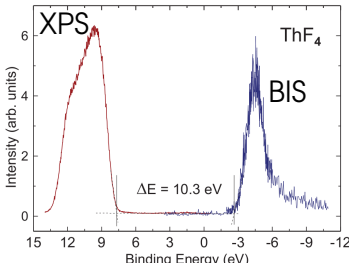
<sup>1</sup> J.K.Ellis et al., Inorg.Chem.53 (2014) 6769



<sup>t</sup> used in thoriumclock.eu project

# ThF<sub>4</sub> bandgap measurements (JRC, Karlsruhe)

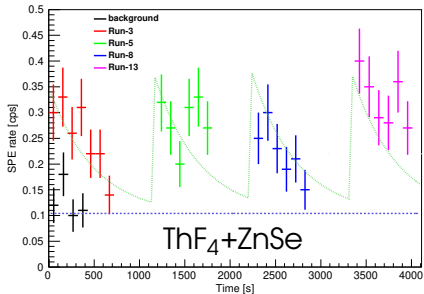
- 1 25 nm film of ThF<sub>4</sub> grown on Au substrate,
- 2 XPS measured valence band,
- 3 BIS measured conduction band,
- 4 REELS confirmed XPS-BIS results,
- 5  $E_g = 10.2 \pm 0.2$  eV,
- 6 > 8.3 eV, suitable for nuclear clock matrix.



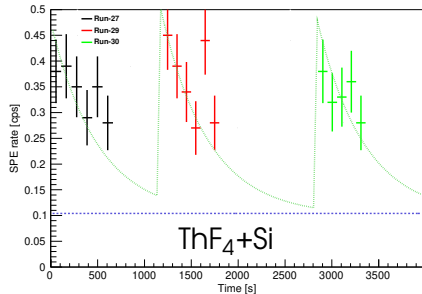
# UV photo-luminescence of ThF<sub>4</sub>

- 0.2 Hz UV photo-lumi. observed on top of 0.1 Hz flat background (opposite side lumi. =bkg.) ✓,
- UV photo-lumi. decay time of about 400 s ✗,
- light yield from ThF<sub>4</sub>+Si sample was larger by factor 3/2 in agreement with ThF<sub>4</sub> layer thickness ratio ✓,
- does not depend on irradiation time (Run.30 after 15 min. irradiation should have 1.85 times higher lumi.) ✓,
- previous item demonstrates that the excitation process is different from the decay.

*M.Osipenko et al., NIM A 1068 (2024) 169744*



ThF<sub>4</sub>+ZnSe



ThF<sub>4</sub>+Si

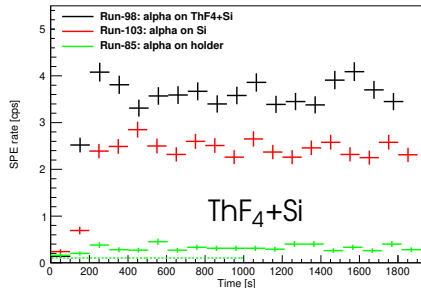
# UV radio-luminescence of ThF<sub>4</sub>

- 1.2 Hz UV radio-lumi. observed (opposite side lumi. subtracted) on top of 0.1 Hz background ✓,
- light yield from ThF<sub>4</sub>+ZnSe sample =0.8 Hz was smaller by factor 3/2 in agreement with ThF<sub>4</sub> layer thickness ✓,
- 1.4 kBq <sup>241</sup>Am source placed 2 mm above the sample, provides 0.4 kHz of  $\alpha$ s on ThF<sub>4</sub> film,
- mean  $\alpha$  energy loss in 300 nm of ThF<sub>4</sub> film was 126 keV and PMT acceptance of about 0.1 gives:  
 $1.7 \times 10^{-3} / EQ(\lambda)$  UV-photons(120-200 nm)/keVee ✓.

$\alpha$ -source above sample



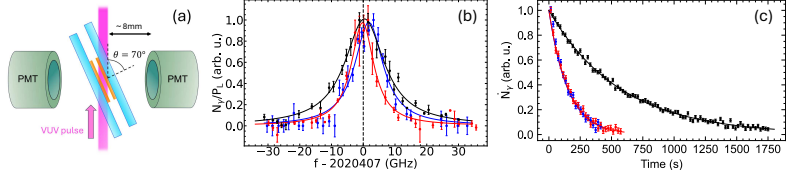
[M.Osipenko et al., NIM A 1068 \(2024\) 169744](#)



# $^{229m}$ Th excitation in $^{229}\text{ThF}_4$ thin films

- 30 nm thin film of (21 kBq)  $^{229}\text{ThF}_4$  was grown on  $\text{MgF}_2$  and  $\text{Al}_2\text{O}_3$  ✓,
- $^{229m}$ Th excitation was observed at  $2020406.8(4)_{\text{stat}}(30)_{\text{sys}}$  GHz ✓,
- $\gamma$ -decay of photo-excited  $^{229m}$ Th in  $\text{ThF}_4$  was observed ✓,
- $^{229m}$ Th lifetime in  $\text{ThF}_4$  of  $153(9)_{\text{stat}}(7)_{\text{sys}}$  s was measured ✓.

C.Zhang et al., Nature 636 (2024) 603



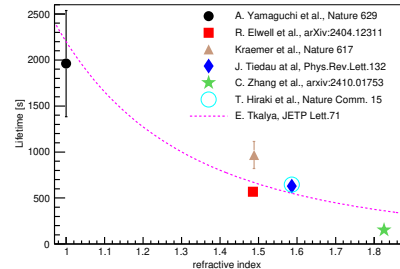
# $^{229m}\text{Th}$ lifetime medium dependence

- predicted  $^{229m}\text{Th}$  lifetime dependence on the medium refractive index  $n^*$ :

$$\tau_{\text{med}} = \frac{\tau_{\text{vac}}}{n^3},$$

- measured lifetimes of  $^{229m}\text{Th}$  are decreasing with  $n$  ✓,
- but lifetime in  $\text{ThF}_4$  is 2.4 times smaller than expected,
- could be due to small thickness of the  $\text{ThF}_4$  film,
- this may allow to manipulate  $^{229m}\text{Th}$  lifetime in thin films.

M.Osipenko et al., NIM A 1068 (2024) 169744



$$t_{\text{ThF}} \simeq 30 \text{ nm} \ll \lambda_0 \simeq 150 \text{ nm},$$

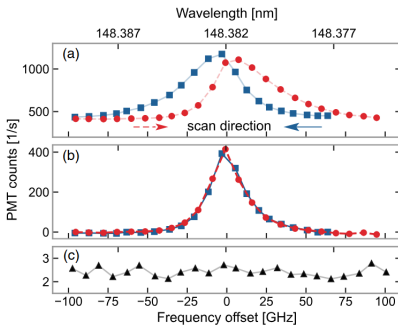
$$\tau_{\text{ThF4}} \simeq 153 \text{ s}$$

$$\tau_{\text{ThF4--expected}} \simeq 361 \text{ s}$$

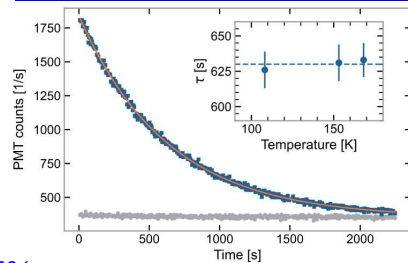
\*E. Tkalya, JETP Lett. 71 (2000) 311

# $^{229m}$ Th excitation in CaF<sub>2</sub> bulk

- $\geq 1 \text{ mm}^3$  CaF<sub>2</sub> crystals with  $10^{-5} \div 10^{-3}$  (w.r.t. Ca) concentration  $^{229}\text{Th}$  doping were grown ✓,
- $^{229m}\text{Th}$  excitation was observed at 148 nm ✓,
- $\gamma$ -decay of hadro<sup>1</sup>- and photo-excited  $^{229m}\text{Th}$  was observed ✓,
- $^{229m}\text{Th}$  lifetime in ThF<sub>4</sub> of 630(15) s was measured ✓.



J. Tiedau et al., PRL 132 (2024) 182501



T. Hiraki et al., Nature Comm. 15 (2024) 5536

S. Kraemer et al., Nature 617 (2023) 706

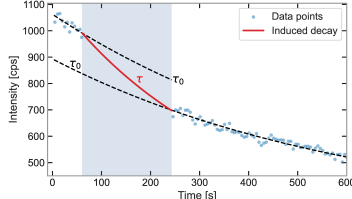
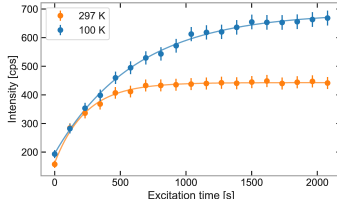
C. Zhang et al., Nature 633 (2024) 63

# Quenching of $^{229m}\text{Th}$ decay in $\text{CaF}_2$

$^{229m}\text{Th}$  lifetime quenching was observed varying crystal temperature and irradiating it with CW laser:

- 2.6 times quenching was observed at  $T=300\text{ K}$  w.r.t.  $T=100\text{ K}$  ✓,
- 3 times quenching was observed irradiating crystal by  $\leq 420\text{ nm}$  CW laser beam of  $20\text{ mW}$  ✓,
- quenching may allow to reduce nuclear clock cycle times,
- shorter cycle time improves frequency stability and important for new physics searches<sup>1</sup>.

*F. Schaden et al., arxiv:2412.12339 (2024)*



<sup>1</sup> M.S. Safronova et al., Rev.Mod.Phys. 90 (2018) 025008

# Solid State Nuclear Clock

- $^{229}\text{Th}^{4+}$  ion embedded in crystal,
- crystal bandgap  $>8.3$  eV suppresses IC.

Pros:

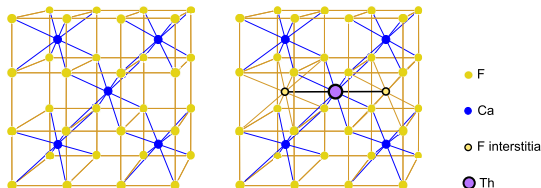
- ① very high number of oscillators ( $10^{19} \text{ cm}^{-3}$ ,  $>10$  orders of magnitude above ion traps) ✓,
- ② stable, easy to handle solid state target ✓,
- ③ no first-order Doppler effect even at room temperature, recoil energy is far below the energy required for creating a phonon ✗.

Cons:

- ① Zeeman interaction between  $^{229}\text{Th}$  with nearby F nuclei and second-order Doppler effect ✗.

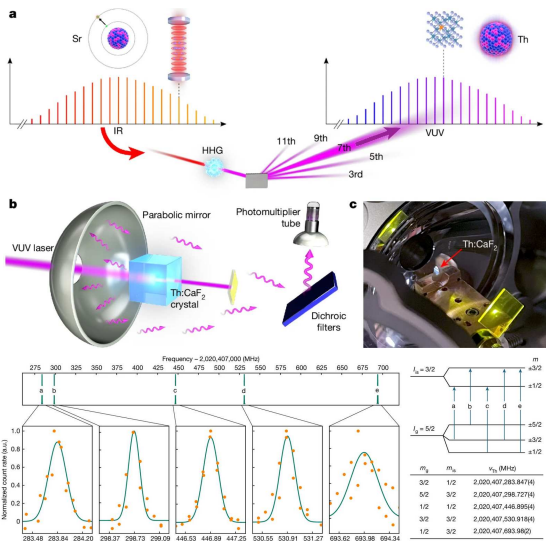
<sup>1</sup> [G.Kazakov et al., New J.Phys. 14 \(2012\) 083019](#)

<sup>2</sup> [W.Rellergert et al., Phys.Rev.Lett. 104 \(2010\) 200802](#)



# First Prototype

- $^{87}\text{Sr}$  atomic clock IR beam generated 7th harmonic for  $^{229m}\text{Th}$  excitation ✓,
- $^{229m}\text{Th}$  quadrupole splitting was observed ✓,
- 300 kHz FWHM ( $1.6 \times 10^{-10}$ ) linewidth of VUV-comb ✗,
- 2 kHz ( $10^{-12}$ ) precision on frequency of  $^{229m}\text{Th}$  achieved by a fit of five quadrupole lineshapes ✗.

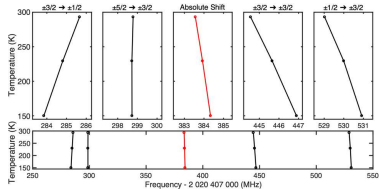
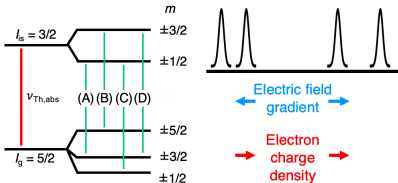


# Temperature-dependent line shift

Absolute frequencies of the electric quadrupole splitting structure of  $^{229m}\text{Th} \rightarrow ^{229g}\text{Th}$  transition in  $\text{CaF}_2$  crystal:

- observed in average MHz/K temperature drift **X**,
- only  $m = \pm 5/2 \rightarrow \pm 3/2$  transition shows 0.4 kHz/K drift **✓**,
- 5  $\mu\text{K}$  temperature stability required to reach  $10^{-18}$  precision.

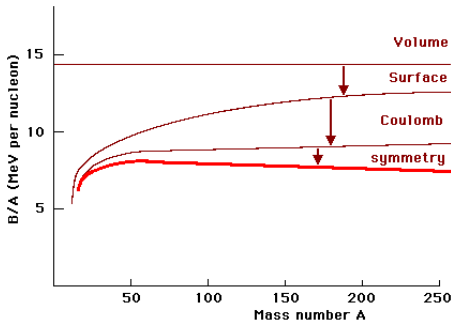
*J.S. Higgins et al., arxiv:2409.11590 (2024)*



# Variations of $\alpha_{EM}$ (with respect to $\alpha_S$ )

- Unification theories applied to cosmology suggest a possibility of variation of the fundamental constants in the expanding Universe , ▶ J.P. Uzan, Rev.Mod.Phys.75 (2003) 403
- searches temporal variation of  $\alpha_{EM}$  in comparison of atomic transitions reached limit  $\frac{1}{\alpha} \frac{d\alpha}{dt} < 10^{-16}/\text{year}$ ,
- increase sensitivity using large nuclear Coulomb energies ( $E_C \sim \text{few MeV}$ ), ▶ V. Flambaum Phys.Rev.Lett.97 (2006) 092502

$$\frac{\delta\nu}{\nu} \simeq k \frac{\delta\alpha}{\alpha}, \text{ with } k = \frac{\Delta E_C}{\nu}$$



# Variations of $\alpha_{EM}$ (with respect to $\alpha_S$ ) cont.

- first estimates gave very optimistic results:

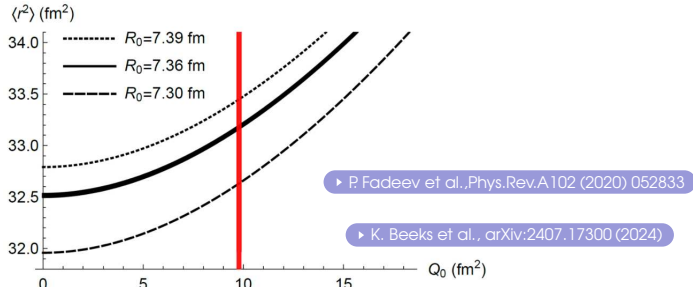
$$\frac{\delta\nu}{\nu} \simeq (k = 10^5) \times \left[ 4 \frac{\delta\alpha}{\alpha} + \frac{\delta X_q}{X_q} - 10 \frac{\delta X_s}{X_s} \right], \quad X_{q,s} = \frac{m_{q,s}}{\Lambda_{QCD}}, \quad k = \frac{\Delta E_C}{E_{iso}}$$

leading to sensitivity:

► V. Flambaum Phys.Rev.Lett.97 (2006) 092502

$$\frac{1}{\alpha} \frac{d\alpha}{dt} \simeq 10^{-20}/\text{year} \ll 10^{-17}/\text{year}(\text{current}) ,$$

- most recent estimate, based on  $^{229}\text{Th}$  charge radii gave  $k \simeq (5.9 \pm 2.3) \times 10^3$ , leading to  $\delta\nu < 100 \text{ Hz/year}$ .



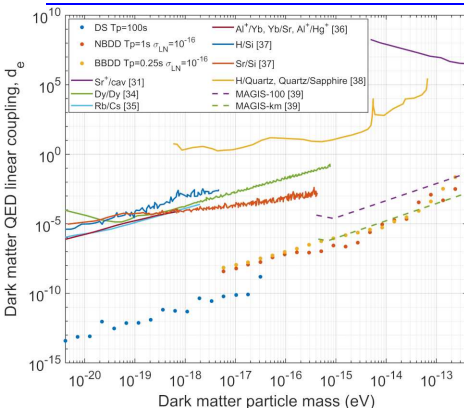
# Ultra Light Dark Matter search

- coupling of ULDM to SM leads to oscillations of fundamental constants (e.g.  $\alpha_{EM}$ ), <sup>1</sup>[arXiv:2203.14915 \(2022\)](https://arxiv.org/abs/2203.14915).
- transient changes in fundamental constants may be induced by DM with large spatial extent<sup>1</sup>,
- comparison of  $^{229m}\text{Th}$  nuclear clock to optical lattice clock allows highest sensitivity.

Schemes:

- 1 Differential Spectroscopy (DS),
- 2 Narrowband Dynamical Decoupling (NBDD),
- 3 Broadband Dynamical Decoupling (BBDD).

[M.H. Zaheer et al., arXiv:2302.12956 \(2023\)](https://arxiv.org/abs/2302.12956)



# Other $^{229m}\text{Th}$ applications

- ①  $^{229m}\text{Th}$ -based current-induced  $\gamma$ -source:  
E.V. Tkalya et al., Chin.Phys.C47 (2023) 024101
- ②  $^{229m}\text{Th}$ -based nuclear laser:  
Zeeman splitting in 100 T magnetic field;  
E.V. Tkalya, Phys.Rev.Lett. 106 (2011) 162501
- ③ GPS (precision 3-5 m) main uncertainties:  
atmospheric disturbance, clock synchronization and stability, satellite position;
- ④ Chronometric geodesy:  $\Delta\nu/\nu = \Delta U/c^2$   
 $10^{-19}$  clock geodesy at 1 mm, earthquake prediction, search for natural resources, tests of general relativity, clock-based gravitational wave detection.

For review see:

P.G. Thirolf et al., Eur.Phys.J.Spec.Top.233 (2024) 1113

L. von der Wense and B. Seiferle, Eur.Phys.J. A56 (2020) 277

# Summary

- $^{229m}\text{Th}$  is the lowest known nuclear isomer,
- its energy lies around 8.3 eV, corresponding to 150 nm wavelength, accessible with VUV-lasers ✓,
- neutral  $^{229m}\text{Th}$  atom decays through IC in  $7 \pm 1 \mu\text{s}$  ✗,
- $^{229m}\text{Th}$  IC decay is suppressed by ionization or chemical binding ✓,
- $^{229m}\text{Th}^+$  decays by  $\gamma$ -decay in about 2000 s ✓,
- $^{229m}\text{Th}^+$   $\gamma$ -decay lifetime depends on the medium refractive index ( $1/n^3$ ) and on crystal thickness,
- $^{229m}\text{Th}^+$   $\gamma$ -decay linewidth is suitable for very precise nuclear clock ( $10^{-19}$  precision on a single atom in cooled trap,  $10^{-17}$  precision on a single atom in crystal) ✓,
- first prototype of solid state nuclear clock has been tested ( $\delta\nu/\nu \sim 10^{-10}$ ) ✓,
- more promising thin film  $^{229}\text{ThF}_4$  is under development.

- L. von der Wense et al., "Direct detection of the  $^{229}\text{Th}$  nuclear clock transition", Nature 533, 47 (2016),
- J. Thielking et al., "Laser spectroscopic characterization of the nuclear-clock isomer  $^{229\text{m}}\text{Th}$ ", Nature 556, 321 (2018),
- B. Seiferle et al., "Energy of the  $^{229}\text{Th}$  nuclear clock transition", Nature 573, 243 (2019),
- T. Masuda et al., "X-ray pumping of the  $^{229}\text{Th}$  nuclear clock isomer", Nature 573, 238 (2019),
- Kjeld Beeks et al., "The thorium-229 low-energy isomer and the nuclear clock", Nature Reviews Physics 3, 238 (2021),

- S. Kraemer et al., "Observation of the radiative decay of the  $^{229}\text{Th}$  nuclear clock isomer", Nature 617, 706 (2023),
- Adriana Pálffy, "Photon lights a path towards a nuclear clock", Nature 617, 706 (2023),
- Atsushi Yamaguchi et al., "Laser spectroscopy of triply charged  $^{229}\text{Th}$  isomer for a nuclear clock", Nature 629, 62 (2024),
- Takahiro Hiraki et al., "Controlling  $^{229}\text{Th}$  isomeric state population in a VUV transparent crystal", Nature Communications 15, 5536 (2024),
- C. Zhang et al., "Frequency ratio of the  $^{229m}\text{Th}$  nuclear isomeric transition and the  $^{87}\text{Sr}$  atomic clock", Nature 633, 63 (2024),

-  C. Zhang et al., " $^{229}\text{ThF}_4$  thin films for solid-state nuclear clocks", Nature 636, 603 (2024).

-  B.R. Beck et al., "*Energy splitting of the ground-state doublet in the nucleus  $^{229}\text{Th}$* ", Phys. Rev. Lett. 98, 142501 (2007).
-  W. G. Rellergert et al., "*Constraining the evolution of the fundamental constants with a solid-state optical frequency reference based on the  $^{229}\text{Th}$  nucleus*", Phys. Rev. Lett. 104, 200802 (2010).
-  W.T. Liao et al., "*Coherence-enhanced optical determination of the  $^{229}\text{Th}$  isomeric transition*", Phys. Rev. Lett. 109, 262502 (2012).
-  X. Zhao et al., "*Observation of the Deexcitation of the  $^{229m}\text{Th}$  Nuclear Isomer*", Phys. Rev. Lett. 109, 160801 (2012).

-  E. Peik and K. Zimmermann, "Comment on Observation of the Deexcitation of the  $^{229m}\text{Th}$  Nuclear Isomer", Phys. Rev. Lett. 111, 018901 (2013).
-  J. Jeet et al., "Results of a Direct Search Using Synchrotron Radiation for the Low-Energy  $^{229}\text{Th}$  Nuclear Isomeric Transition", Phys. Rev. Lett. 114, 253001 (2015).
-  A. Yamaguchi et al., "Energy of the  $^{229}\text{Th}$  nuclear clock isomer determined by absolute  $\gamma$ -ray energy difference", Phys. Rev. Lett. 123, 222501 (2019).
-  T. Sikorsky et al., "Measurement of the  $^{229}\text{Th}$  isomer energy with a magnetic microcalorimeter", Phys. Rev. Lett. 125, 142503 (2020).
-  J. Tiedau et al., "Laser excitation of the Th-229 nucleus", Phys. Rev. Lett. 132, 182501 (2024).

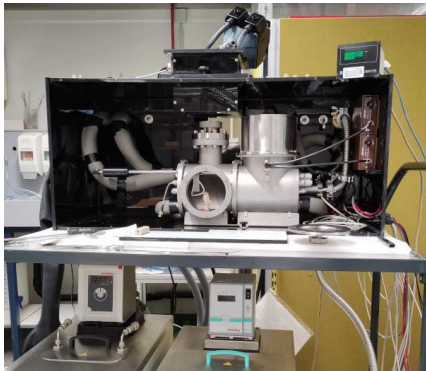
-  R. Elwell et al., "Laser excitation of the  $^{229}\text{Th}$  nuclear isomeric transition in a solid-state host", Phys. Rev. Lett. 133, 013201 (2024).

-  T. Gouder et al., "Measurements of the band gap of ThF<sub>4</sub> by electron spectroscopy techniques", Phys. Rev. Research 1, 033005 (2019),
-  M. Fedkevych et al., "Direct Search for Low Energy Nuclear Isomeric Transition of Th-229m With TES Detector", IEEE T. Appl. Supercon., Vol. 31, No. 5, 2100904 (2021),
-  M. Fedkevych et al., "An Examination of Thermal Coupling of an Ir/Au TES for TORIO-229 Experiment", J. Low Temp. Phys. 209, 473 (2022),
-  M. Osipenko et al., "Measurement of photo- and radio-luminescence of thin ThF<sub>4</sub> films", Nucl. Instrum. Methods A 1068, 169744 (2024).

# Backup slides

# GRaDeTh229 setup at JRC (Karlsruhe)

- ① Hamamatsu VUV-lamp L11798 (120-170 nm),
- ② solar-blind PMT R6835 (115-200 nm) + visible veto PMT R1450 (300-650 nm), CAEN DT5533 power supply,
- ③ charge sensitive amplifiers Ortec 113 and digitizer CAEN DT5730 with PHA firmware,
- ④ vacuum chamber for  $10^{-4}$  mbar,
- ⑤ chiller capable to cool to  $-40\text{ C}^{\circ}$ ,
- ⑥ 2 commercial (amorphous)  $\text{ThF}_4$  samples from II-VI Inc.



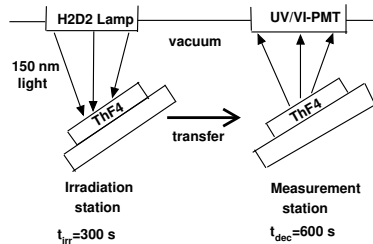
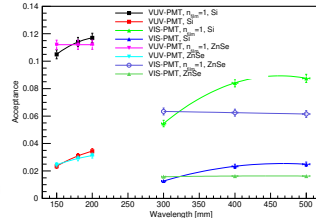
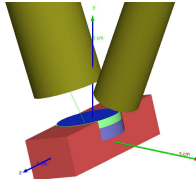
# Method of photo-luminescence measurements

- ① H2D2 VUV-lamp yields:  
 $\sim 10 \mu W/nm$  at 150 nm,
- ② it will excite defects/impurities in  $ThF_4$  crystal layer;
- ③ after transfer we observe:

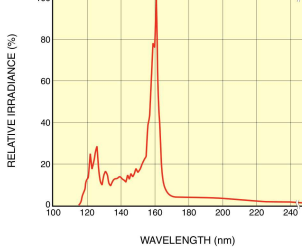
$$Sig = N_{dec} \times Acc \times Eff$$

- ④ acceptance  $Acc \sim 0.03$ ,  
efficiency  $Eff \sim 0.1 \div 0.2$ .

Geant4 simulation

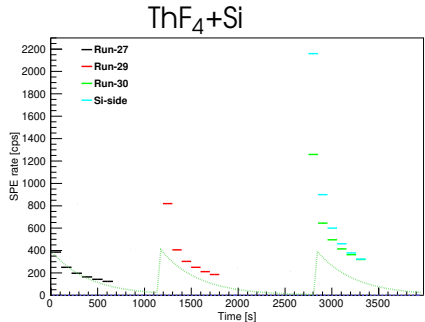
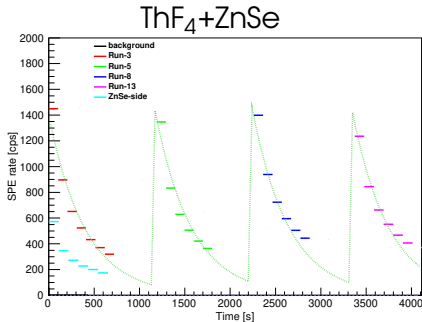


H2D2 emission spectrum



# Visible photo-luminescence of ThF<sub>4</sub>

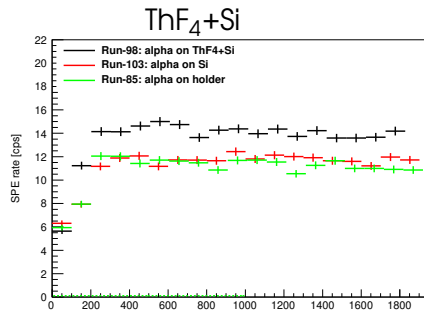
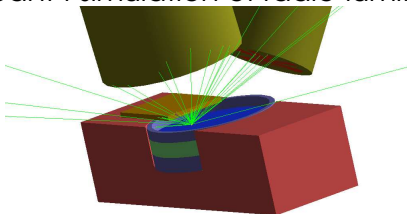
- 0.8 kHz vis. photo-lumi. observed on top of 2.5 Hz noise and 0.6 kHz opposite side lumi.,
- Visible photo-lumi. decay time of 400 s **X**,
- projected accidental rate in 100 ns:  $<10^{-5}$  Hz **✓**,
- on Si sample lumi. build-up was observed over time: humidity entered during sample change?
- first run on Si sample showed lower luminescence: 0.4 kHz vs  $0.8 \pm 0.2$  kHz **X**.



# Visible radio-luminescence of ThF<sub>4</sub>

- 2.3 Hz vis. radio-lumi. observed in ThF<sub>4</sub> on top of 2.5 Hz noise ✓,
- light yield from ThF<sub>4</sub>+ZnSe sample was much larger since ZnSe is a high light yield scintillator, the subtraction of ZnSe-component was not very precise,
- comparison to Geant4 simulation shows that a similar event rate is obtained at ThF<sub>4</sub> light yield of: 0.1 photons/keV (0.7 ph/keVee assuming CaF<sub>2</sub> light quenching =0.15).

Geant4 simulation of radio-lumi.



# Consequences for $^{229m}\text{Th}$ $\gamma$ -decay search

- ① H2D2-lamp at 150 nm yields:  $\sim 10 \mu\text{W/nm}$ , measured  $1.6 \times 10^{13} \text{ 1/cm}^2\text{s nm}$ ,
- ② it will excite  $^{229m}\text{Th}$ :

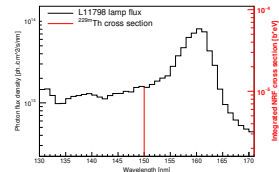
$$\frac{dN_{Th229m}}{dt} = n_{Th229} \frac{1}{3} \frac{n_{ThF_4}^3}{2} \Gamma_\gamma \lambda_0^2 \frac{dN_\gamma}{dE},$$

- ③ for  $n_{Th229}=1 \text{ kBq}/1 \text{ cm}^2$  gives 6.5 Hz:

$$N_{decay} = \frac{dN_{Th229m}}{dt} \tau \left(1 - e^{-\frac{t_{irr}}{\tau}}\right) \left(1 - e^{-\frac{t_{dec}}{\tau}}\right)$$

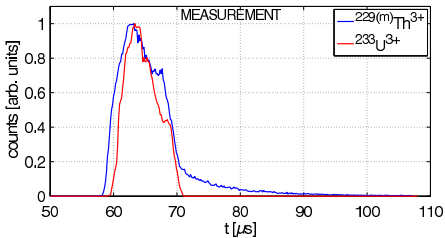
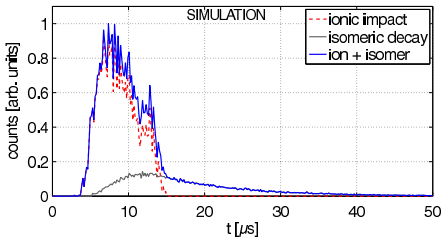
$$R = \frac{N_{decay} \times Acc \times Eff}{\tau} \sim \frac{1780 \times 0.27 \times 0.1}{500 \text{ s}} \sim 0.1 \text{ Hz}.$$

- ④ UV photo-lumi. of  $\text{ThF}_4$ :  
 $0.2 \text{ Hz}/(300 \text{ nm} \times 4.8 \text{ cm}^2)$  for  
 $50 \text{ nm}/1 \text{ cm}^2 = 0.007 \text{ Hz}$  ✓,
- ⑤ UV radio-lumi. of  $\text{ThF}_4$ :  
 $1.2 \text{ Hz}/(300 \text{ nm} \times 0.4 \text{ kBq})$  for  
 $25 \text{ nm} \times 1 \text{ kBq} = 0.27 \text{ Hz}$  ( $\times 5$  for full chain) ✓.



# LMU $^{229m}\text{Th}$ lifetime measurement (2017)

- 1 Extension of direct observation experiment<sup>1</sup>,
  - 2 long  $^{229m}\text{Th}^{3+}$  ion transport (90 ms),
  - 3 fast decay after impact onto MCP (neutralization),
  - 4 neutral  $^{229m}\text{Th}$  lifetime (IC)<sup>2</sup>:  $7 \pm 1 \mu\text{s}$ ,
  - 5 9 orders of magnitude lower than expected ( $\gamma$ ): 1 h,
  - 6 relative linewidth (IC):  $\sim 10^{-11}$  (atomic clock  $< 10^{-13}$ ),
  - 7 neutral  $^{229m}\text{Th}$   $\gamma$ -decay branching:  $\sim 10^{-9}$  (theor.).

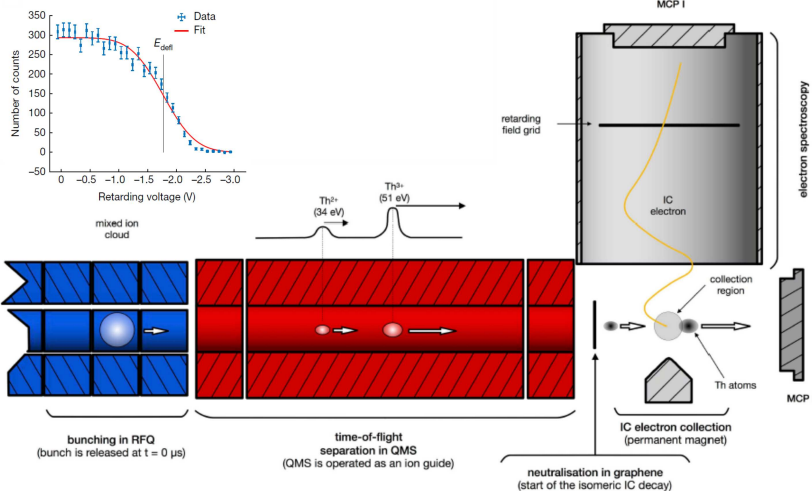


<sup>1</sup>L.von der Wense et.al.Nature 533,47(2016),

<sup>2</sup>B.Seiferle et.al.*Phys.Rev.Lett.* 118,042501(2017).

# LMU $^{229m}\text{Th}$ energy measurement (2019)

measured  $1.77 \text{ eV} + 6.51 \text{ eV}$  (binding) =  $8.28 \pm 0.17 \text{ eV}$



<sup>1</sup>B. Seiferle et al., Nature 573, 243 (2019).

# Previous $^{229m}\text{Th}$ $\gamma$ -decay search

- IC decay has broad linewidth:

$$\frac{\Delta\nu}{\nu} \simeq \frac{1.4 \times 10^5 \text{ Hz}}{2 \times 10^{15} \text{ Hz}} \simeq 10^{-10},$$

- $\gamma$ -decay in neutral atom:

$$\frac{\Gamma_\gamma}{\Gamma_{IC}} \simeq \frac{1/1h}{1/7\mu\text{s}} \simeq 2 \times 10^{-9},$$

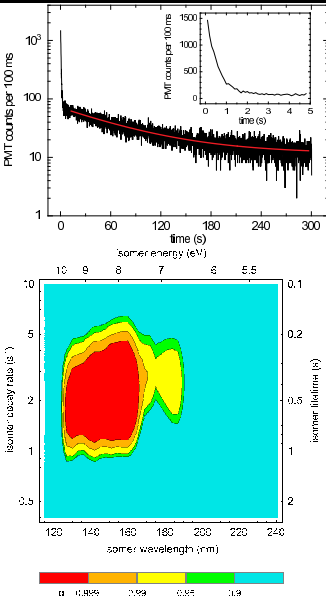
- 1 Th<sup>n+</sup> ion traps ( $10^6$  Th/cm<sup>3</sup>):

$$\sigma_{\gamma abs} \sim 10^{-11} \text{ cm}^2 \frac{3 \times 10^{-19} \text{ eV}}{\Delta\nu_{source}}$$

$$R_{\gamma dec} \sim \rho X \sigma_\gamma \frac{n_\gamma}{\tau_\gamma \sim 1h} \sim \frac{10^2}{s} \frac{\Gamma_\gamma}{\Delta\nu_{source}}$$

- 2 wide bandgap crystals with

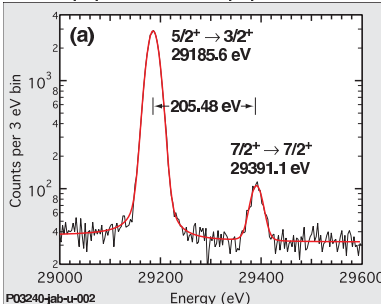
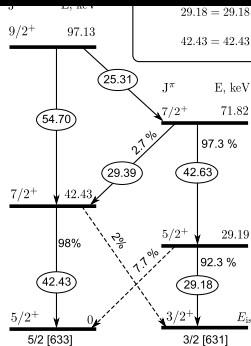
$^{229}\text{Th}$ :  $\text{CaF}_2^1$ ,  $\text{MgF}_2$ ,  
 $\text{LiSrAlF}_6$ ,  $\text{LiCaAlF}_6$



<sup>1</sup>S.Stellmer et.al.Phys.Rev.A97 (2018) 062506.

# Energy level of $^{229m}\text{Th}$ isomer

- 1 indirect measurement<sup>1</sup> by comparison of 43+29 keV  $\gamma$ s with 26 eV resolution (HgTe  $\mu$ calorimeter with 3 ms decay time),
- 2  $100 \mu\text{Ci}^{233}\text{U}$  source covered by  $50 \mu\text{m}$  Ti foil at 3.5 cm distance,
- 3 direct search at ALS<sup>2</sup> with  $^{229}\text{Th}$ -doped  $\text{LiSrAlF}_6$  crystal excluded  $\gamma$ -decay in the region:  $1 - 2 < \tau < 2000 - 5600$  s for  $7.3 < E_\gamma < 8.8$  eV at 90 CL,
- 4 MCP counting observation<sup>3</sup>, obtained upper limit  $< 18.3$  eV.



<sup>1</sup>B. Beck et.al. Phys. Rev. Lett. 98, 142501(2007).

<sup>2</sup>J. Jeet et.al. Phys. Rev. Lett. 114, 253001(2015).

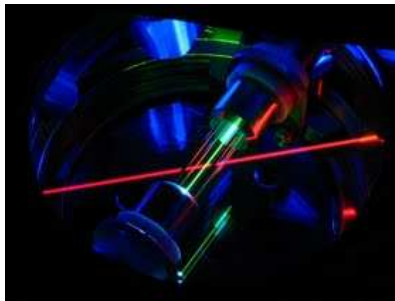
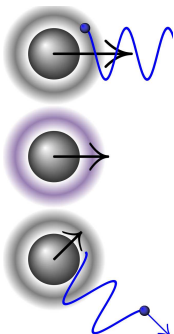
<sup>3</sup>L.von der Wense et.al. Nature 533, 47(2016).

- ① ion trap for  $^{229}\text{Th}^{3+}$ ,
- ② laser cooling,
- ③ laser ablation source,
- ④ low number of oscillators ( $< 10^5$ ),
- ⑤ 100 s trapping lifetime,
- ⑥ measurement of hyperfine structure of  $^{229}\text{Th}^{3+}$  atom.

<sup>1</sup>A.Radnaev et al., *Phys.Rev.A* 86, 060501(R) (2012).

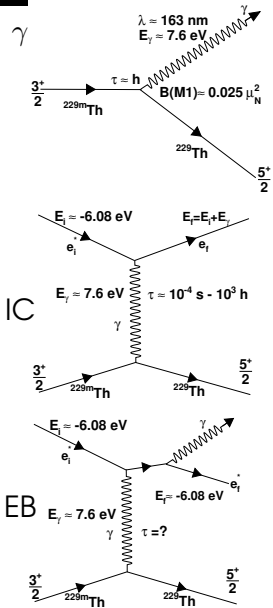
<sup>2</sup>N.Huntemann et al., *Phys.Rev.Lett.* 116, 063001 (2016).

A.Kuzmich, [sites.lsa.umich.edu/kuzmich-lab/](http://sites.lsa.umich.edu/kuzmich-lab/)  
E.Peik, [www.ptb.de/cms/en/ptb/fachabteilungen/abt4/fb-44/ag-443.html](http://www.ptb.de/cms/en/ptb/fachabteilungen/abt4/fb-44/ag-443.html)



# TORIO-229 proposal (CSN3 meeting 22/06/2016)

- 1 Direct measurement of  $^{229}\text{Th}$  lowest level energy and lifetime in the region 5-50 eV and 1 ms-1 h,
- 2 sum of all possible decay channels:  $\gamma$ , IC and EB,
- 3 cryogenic  $\mu$ calorimeter with < 3 eV threshold and <0.5 eV resolution,
- 4  $^{233}\text{U}$ ,  $^{229}\text{Th}$  and  $^{228}\text{Th}$  deposits,
- 5 background studies with  $^{238}\text{U}$  and  $^{232}\text{Th}$  samples,
- 6 signal studies with  $^{235m}\text{U}$  (77 eV, 26 m, E3),  $^{239}\text{Pu}$  deposit.



# $\mu$ calorimeter with embedded source (2016)

Cryogenic  $\mu$ calorimeter heat capacity budget:

- ① 3.8 ng  $^{233}\text{U}$  target 17.3 fJ/K,
- ② Ir TES 8 fJ/K,
- ③ Au absorber 0 fJ/K,
- ④ Si membrane 0.013 fJ/K.

Energy resolution:

$$\sigma_E \sim \sqrt{kT^2 C} \sim 0.42\text{eV} .$$

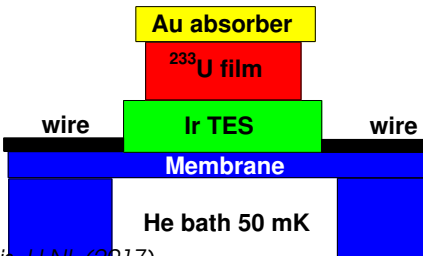
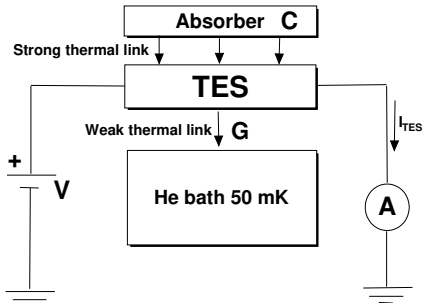
Energy dynamic range 160 eV:

$$\Delta T \sim \frac{E_{dep}}{C} < 1\text{mK} .$$

Target activity: 3.8 ng  $^{233}\text{U}$ ,  
1.3 Bq  $\alpha$  activity ( $A = 0.35 \times M_U[\text{ng}]$ ),  
or 100  $^{229m}\text{Th}/\text{h}$ .

Signal decay time:

$$\tau_D \sim \frac{C}{G} \sim 2.5\text{ms}$$
 F. Ponce, PhD thesis, LLNL (2017).



# $\mu$ calorimeter pile-up

Updated decay rate estimate:

- ① 3.8 ng  $^{233}\text{U}$  target ( $10^{13}$  atoms)
- ② 1.3 Bq  $\alpha$  activity  
( $A = 0.35 \times M_U [\text{ng}]$ ),
- ③ 100  $^{229m}\text{Th}/\text{h}$ ,
- ④  $10^{-3} \, ^{229m}\text{Th} \gamma$  decay/y.

Signal decay time:

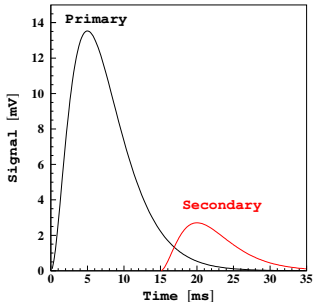
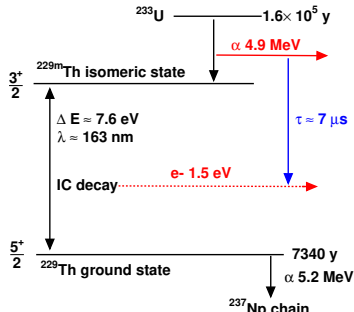
$$\tau_D \sim \frac{C}{G} \sim 2.5 \text{ ms} .$$

Separation of two decays:

$$\Delta t > \tau_D \ln \frac{E_{\text{primary}}}{E_{\text{secondary}}} .$$

Probability of separated decay:

$$P \sim \exp \left[ -\frac{2.5 \text{ ms}}{7 \mu\text{s}} \right] \sim 10^{-155} .$$

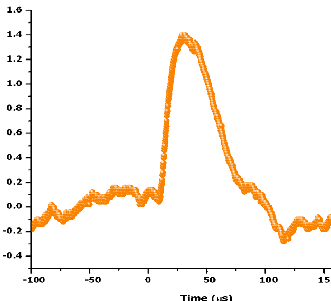
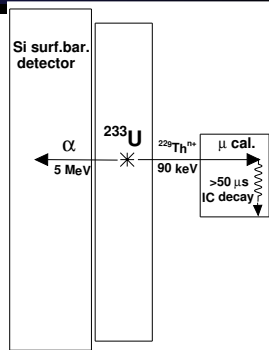


# TORIO-229 setup (CSN3 meeting 22/06/2017)

- Fast cryogenic pyrochronometer with signal full decay time  $\Delta t < 50 \mu\text{s}^1$ ,
- $\alpha$ - $^{229}\text{Th}^+$  coincidence,
- $^{233}\text{U}$  deposited on Si detector,
- long. range of 90 keV  $^{229}\text{Th}^+$  in U is 6.7 nm (path 10.7 nm),  
in  $\text{UO}_2$  is 8.3 nm (path 16.1 nm),
- 10 nm thick  $^{233}\text{U}$  film with 1 nm Mg layer or 20 nm thick  $^{233}\text{UO}_2$  film,  
activity  $A_U < 5 \text{ kBq}$ ,
- expected rate of time-separated events (assumes  $t_{IC} = 7 \mu\text{s}$ ):

$$R_{IC}^{\mu\text{cal}} \sim A_U B_{229m} A_{\mu\text{cal}}^{\text{geom}} e^{-\Delta t/t_{IC}},$$

$$R_{IC}^{\mu\text{cal}} \sim 10^4 * 0.02 * 10^{-4} * 10^{-3} \sim \frac{1}{\text{day}}.$$



<sup>1</sup>D.Bagliani et al., J.Low.Temp.Phys. 151, 234(2008).

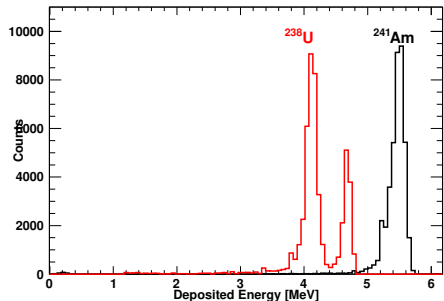
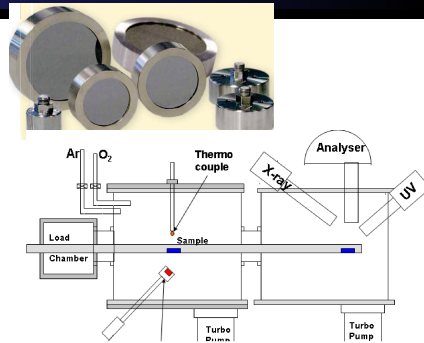
# Primary sources (R. Caciuffo, JRC, Karlsruhe)

First source was deposited by sputtering on active surface of Si detector ( $300\text{ mm}^2$ ), in form of  $\text{UO}_2$  dielectric film with diameter 10mm and thickness 10 nm:

- ①  $^{238}\text{U} < 0.2 \text{ Bq}$  (+0.1 Bq  $^{234}\text{U}$ ), delivered for background measurements,
- ②  $^{233}\text{U} < 5 \text{ kBq}$ , authorization received, waiting for working TES prototype.

Source requirements:

- E-loss limits thickness  $\leq 20 \text{ nm}$ ,
- Si-rate limits activity  $< 40 \text{ kHz}$ .



# $\mu$ calorimeter principles

$\mu$ calorimeter operation:

- ① constant current flows through TES without resistance,
- ② deposited energy is transformed in heat,
- ③ heat increases TES resistance,
- ④ Resistance reduces flowing current,
- ⑤ current read by SQUID.

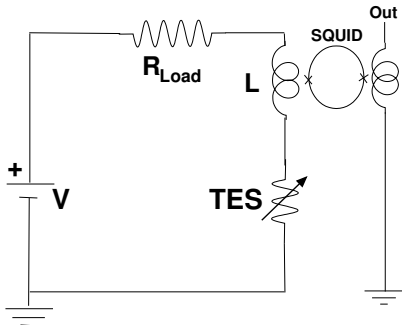
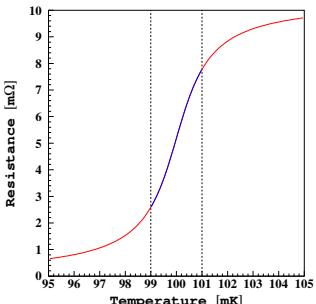
Signal:

$$\Delta T = E_{\text{dep}}/C \sim 2fJ/K .$$

Energy resolution:

$$\sigma_E \sim \sqrt{kT^2 C} .$$

SQUID noise:  $1 \text{ pA}/\sqrt{\text{Hz}}$ .



# $\mu$ calorimeter optimization

- Signal decay time at  $T = 100$  mK:

$$\tau \sim \frac{C_{\text{bottleneck}}}{G \sim 10^5 fW/K} \sim 10 \mu\text{s}.$$

- $T$ -dependence:

$$\frac{C \simeq \gamma V^{\text{large}}}{G \sim G_{ep} \simeq 5 \sum V T^4} = \frac{\gamma}{5 \sum \tau^3}$$

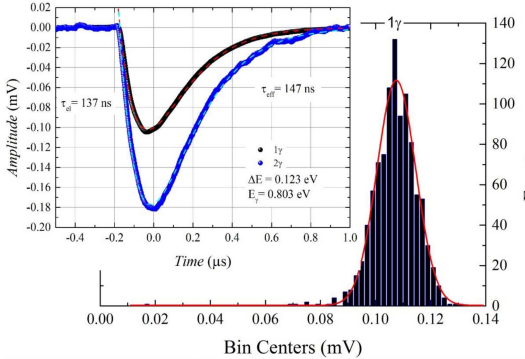
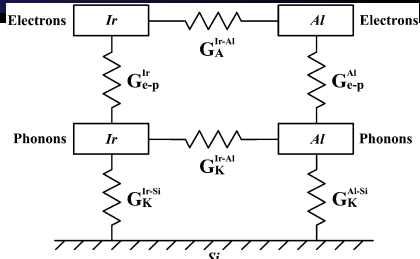
- $T = 100\text{mK} \rightarrow 300\text{mK}$ :

$$\tau(300\text{mK}) \sim \frac{\tau(100\text{mK})}{30}$$

- noise power:

$$NEP \sim \sqrt{4k_b T^2 G},$$

$$V_{noise} \sim [20k_b \Sigma V]^{1/4} T^{3/2}$$

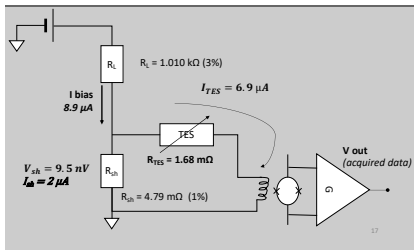
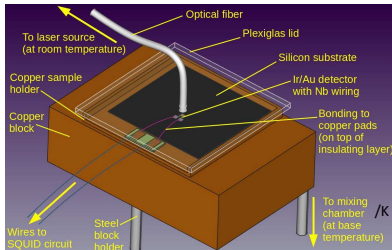
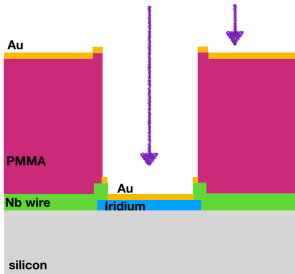


<sup>1</sup>D.Bagliani et al., J.Low.Temp.Phys. 151, 234(2008).

<sup>2</sup>C.Portesi et al., IEEE Trans.App.Supercond. 25, 3(2015).

# TES development details

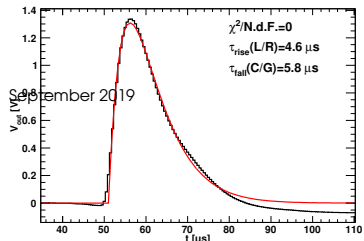
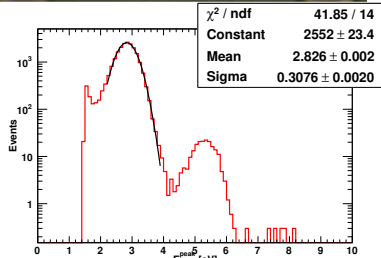
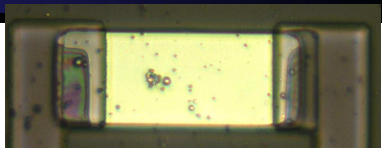
- 1 design lithographic mask,
- 2 tested Ti-Au and Ir TESs,
- 3 tested Nb and Al wiring,
- 4 PLD of Ir, sputtering of Nb,
- 5 PMMA+Au shadow mask<sup>1</sup>,
- 6 wire bonding to SQUID,
- 7 alignment of fiber,
- 8 SQUID calibrations.



<sup>1</sup>M.Fedkevych et al., 10.1109/TASC.2021.3063328

# Detector development and characterization

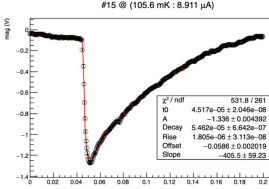
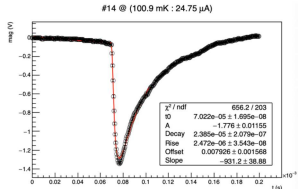
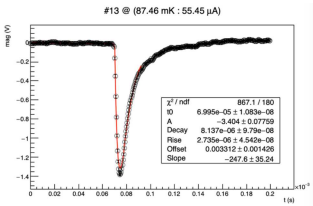
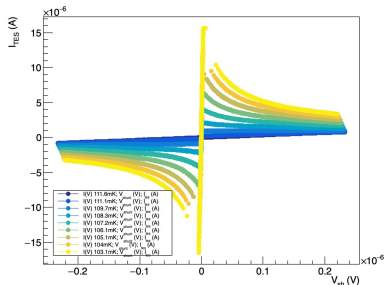
- ① developed Ir TES satisfying experimental requirements<sup>1</sup>: signal fall time  $\tau < 10 \mu\text{s}$ , resolution  $\Delta E < 1 \text{ eV}$ ,
- ②  $15 \times 26 \mu\text{m}^2$ , 150 nm thick Ir,
- ③ few  $\mu\text{m}$  PMMA + 50 nm Au shadow mask,
- ④ transition  $T_c = 110.5 \text{ mK}$ ,
- ⑤ laser calibrations and Poissonian fit,
- ⑥ analysis of data and extraction of TES parameters.



# TES characterization details

- 1 high bias current  $60\mu\text{A}$ ,
- 2 operation at  $90 \text{ mK} < T_C$ ,
- 3 large negative electrothermal feedback<sup>1</sup>:

$$\tau_{\text{eff}} \simeq \frac{\tau_{th}}{1 + \alpha P/GT}.$$



<sup>1</sup> M.Biasotti, internal report (2020).